Effect of valence-band hybridization on the exciton spectra in GaAs-$Ga_{1-x}Al_xAs$ quantum wells

Bangfen Zhu* and Kun Huang
Institute of Semiconductors, Academia Sinica, Beijing, China
(Received 24 April 1987)

An investigation is made into the effect of valence-band coupling on Wannier excitons in GaAs-$Ga_{1-x}Al_xAs$ quantum wells with well widths ranging from 30 to 200 Å. The results of our calculation show that the effect is twofold. On the one hand, hole-subband nonparabolicity due to mixing of the heavy- (HH) and light-hole (LH) states causes an increase in the binding energies E^{ex}, of both ground- and excited-state excitons; on the other hand, the different orbital behaviors of the spinor components of the excitonic wave function result in a decreased E^{ex} of s-state excitons and an increased E^{ex} of p- and d-state excitons. The former effect dominates in narrower wells and the latter effect dominates in wider wells. The two-band model is a good approximation for calculating E^{ex}(HH1), but can cause a significant error in calculating E^{ex}(LH1) in wider wells because of the stronger coupling between exciton states from different subbands.

I. INTRODUCTION

The free-electron and hole carrier states interact through the screened Coulomb potential to form excitons. The complex nature of the hole wave function has an important effect on the exciton state. In a GaAs-$Ga_{1-x}Al_xAs$ quantum well (QW), owing to different effective masses along the axis of growth (referred to as the z axis in this paper), the fourfold degeneracy at the valence-band edge of GaAs is removed with the formation of the so-called heavy- (HH) and light-hole (LH) subband. In the earlier models for the hole subbands, the hole motion along the z axis was considered to be decoupled from its motion in the xy plane and the subbands were thus taken as parabolic. On the basis of such a model, Greene and Bajaj[1] have calculated the exciton binding energies in a QW with potential barrier of finite height.

However, it has been shown[2-5] that the off-diagonal terms of the Luttinger-Kohn Hamiltonian[6] mix the HH and LH states away from $\mathbf{k}=0$, where $\mathbf{k}$ is the wave vector in the plane of the well. This coupling results in large nonparabolicities in the hole subbands. Recently, Sanders and Chang,[7] Broido and Sham,[8] taking the hybridization of the HH and LH states into account, have evaluated the binding energy of the ground state of the first HH exciton E_{1s}^{ex}(HH1), and that of the first LH exciton E_{1s}^{ex}(LH1). The exciton wave function Ψ_{ex} in their works was expressed in terms of a general linear combination of direct products of QW electron and hole eigenstates,

$$\begin{aligned}\Psi_{ex}&=\sum_{\mu,\nu}\sum_{\mathbf{k},\mathbf{k}'}F_{\mu\nu}(\mathbf{k},\mathbf{k}')\psi_{h,\nu}(\mathbf{k},\boldsymbol{\rho}_h,z_h)\psi_{e,\mu}(\mathbf{k}',\boldsymbol{\rho}_e,z_e)\\&=\sum_{\mu,\nu}\sum_{\mathbf{k},\mathbf{k}'}F_{\mu\nu}(\mathbf{k},\mathbf{k}')f_\mu(z_e)e^{i\mathbf{k}'\cdot\boldsymbol{\rho}_e}U_0\\&\quad\times\sum_{j=1}^{4}g^j(\mathbf{k},z_h)U^j e^{i\mathbf{k}\cdot\boldsymbol{\rho}_h}\ .\end{aligned}\tag{1}$$

Here spinor $\psi_{h,\nu}$ is the wave function of the νth hole subband for a given two-dimensional (2D) wave vector $\mathbf{k}$, expressed in cylindrical coordinates $(\boldsymbol{\rho}_h,z_h)$, while $\psi_{e,\mu}$, $\mathbf{k}'$, and $(\boldsymbol{\rho}_e,z_e)$ refer to similar quantities for the electron. $F_{\mu\nu}$ is the exciton envelope function. In the second line of (1), the general form of the electron- and hole-subband wave functions are explicitly displayed, where U^j is the zone-center valence-band Bloch state for spin component $j(=\frac{3}{2},\frac{1}{2},-\frac{1}{2},-\frac{3}{2})$, and U_0 is the zone-center conduction-band Bloch state. Both of the previous works put emphasis on the effect of the hole-subband nonparabolicity on the effective reduced mass of the excitonic state and obtained larger binding energies as compared with the results of Greene and Bajaj.

In actual fact, the valence band coupling also affects significantly the Coulomb interaction between the electron-hole pair, because the different spinor components of the hole-subband wave function correspond to different in-plane angular momenta and lead to characteristically different radial distributions in the exciton structure. As we shall show, this effect is as important as the effect resulting from hole-subband nonparabolicity. Apparently, it has not been properly dealt with in the above cited works. Thus in Ref. 7, in calculating the Coulomb energy $g^j(\mathbf{k},z_h)$ was approximated by $g^j(0,z_h)$, thereby the form of the exciton wave function reduced simply to that of Greene and Bajaj. In Ref. 8, $g^j(\mathbf{k},z_h)$ was taken as $g^j(k,z_h)$, the difference in the angular momenta associated with the spinor components of the exciton wave function was apparently overlooked.

In this paper we intend to evaluate the effect of valence band coupling on the Coulomb energy of the excitons. Since there are not, to our knowledge, any investigations about the binding energies of the excited-state exciton based on the complex-hole subbands, we present a variational calculation of E^{ex} of both ground and a few low-lying states of excitons in QW of finite values of the potential barrier heights. In Sec. II the electron- and hole-subband structures and the character of the hole

states in QW's are reviewed. In Sec. III a method is developed for determining E^{ex}. The numerical results are contained in Sec. IV. Finally, a comparison with experiments and a discussion of various approximations used in the present work are presented.

II. SUBBAND STRUCTURE

In the present work, the electron and hole subbands and the exciton problem will be treated in the effective-mass approximation. The effective mass m_e^* of the electron is taken to be $0.0665m_0$. The Luttinger parameters for the valence band are taken from Ref. 7, namely, $\gamma_1=6.93$, $\gamma_2=2.15$, and $\gamma_3=2.81$. The band-gap mismatch between GaAs and $Ga_{1-x}Al_xAs$ will be taken to be $\Delta E_g=(1.115x+0.37x^2)$ eV (Ref. 9) with barrier height for electron V_e equal to $0.6\Delta E_g$ and barrier height for hole V_h equal to $0.4\Delta E_g$.[10]

The hole subbands are calculated by a method developed by Tang and Huang,[5] which parallels usual pseudopotential energy band calculations in terms of plane-wave basis functions. In the present instance, the usual HH and LH plane wave solutions constitute the basis functions, with a Kronig-Penny–type barrier potential taking the place of the atomic pseudopotentials. A very limited number of reciprocal superlattice vectors mK need be used to obtain reasonable accuracy, where $K=2\pi/(L+d)$ and L and d are the well and barrier widths, respectively. In this formalism, the wave function of the νth hole subband has the following form:

$$\psi_{h,\nu}(\mathbf{k},\rho_h,z_h)=\exp(i\mathbf{k}\cdot\rho_h)\sum_{m=-N}^{N}\sum_{i=1}^{4}a_{m_i}\phi_i(\mathbf{k},mK)\exp(imKz_h)\ , \tag{2}$$

where $\phi_i(\mathbf{k},mK)$ are the usual HH and LH spinor wave functions associated with $\mathbf{k}=k_x+ik_y=k\exp(i\theta)$ and $k_z=mK$, and a_{mi} are expansion coefficients to be determined by solving a $[4(2N+1)]$th-order secular equation. The superlattice wave number in the z direction has been taken to be zero, which is immaterial for quantum wells effectively decoupled. For simplicity, subband anisotropy has been neglected so that the energy dispersion $E(\mathbf{k})$ depends only on k. The solution $\psi_{h,\nu}$ can be written in the following form:

$$\psi_{h,\nu}(\mathbf{k},\rho_h,z_h)=\exp(i\mathbf{k}\cdot\rho_h)\begin{bmatrix}\alpha_\nu(k,z_h)\exp(-i\theta)\\ \beta_\nu(k,z_h)\\ \gamma_\nu(k,z_h)\exp(i\theta)\\ \delta_\nu(k,z_h)\exp(i2\theta)\end{bmatrix}\ , \tag{3}$$

where α_ν,γ_ν are odd and β_ν,δ_ν are even in z_h. Another solution, which is degenerate with (3), is of the form

$$(\delta_\nu\exp(-i\theta),\gamma_\nu,\beta_\nu\exp(i\theta),\alpha_\nu\exp(i2\theta))^T\ .$$

Two points should be noticed.

(1) ψ_h is a spinor with four components, which are generally nonvanishing except at $k=0$. At $k=0$, however, only one component is nonvanishing, thus in our designation, $\psi_{h,\mathrm{HH1}}(k=0)$ has only a $-\frac{3}{2}$ component and $\psi_{h,\mathrm{LH1}}(k=0)$ has only a $\frac{1}{2}$ compnent.

(2) In our model of isotropy approximation, although the energy $E(\mathbf{k})$ does not depend on θ, the wave function ψ_h depends on θ and the different angular factors $\exp(il\theta)$, as we shall see, will lead to different orbital angular momenta in the exciton wave function.

Figure 1 shows a comparison of the subband dispersion curves calculated for a QW of $L=150$ Å with and without the isotropy approximation.

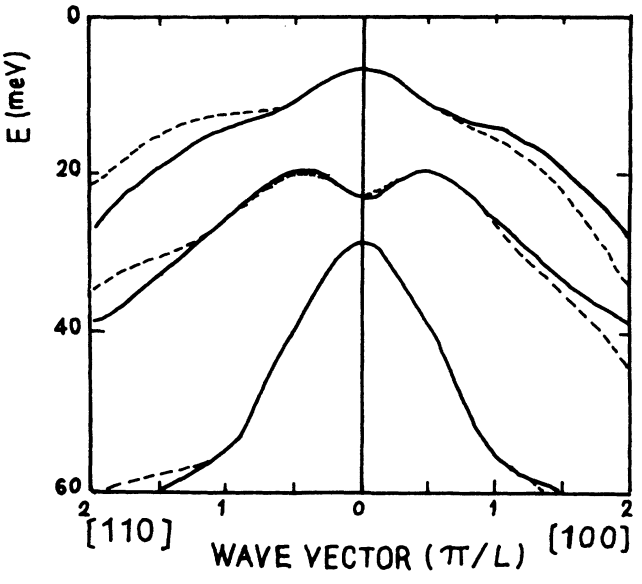

FIG. 1. Calculated are the topmost three hole subbands in a quantum well of $L=150$ Å. The solid curves are for the isotropy approximation and the dashed curves include anisotropy.

III. CONSTRUCTION OF EXCITON WAVE FUNCTION

The Hamiltonian of a Wannier exciton in a QW is given by

$$H_{ex}=H_h+H_e+V_{Coul} \tag{4}$$

with

$$V_{Coul}=-e^2/\epsilon[\rho^2+(z_h-z_e)^2]^{1/2}\ . \tag{5}$$

Here $\rho=\rho_e-\rho_h=\rho\exp(i\varphi)$ and ϵ is the static dielectric constant taken to be 12.5 in this paper.

For a stationary exciton with zero translational momentum, the envelope function as defined in (1) has the following form:

$$F_{\mu\nu}(\mathbf{k},\mathbf{k}')=\delta(\mathbf{k}+\mathbf{k}')G_{\mu\nu}(\mathbf{k}) . \tag{6}$$

The Coulomb interaction couples states from different subbands. However, for sufficiently narrow wells such that the subband energies are well separated and the coupling is weak, we can adopt a two-band model keeping only one valence and one conduction subband. In view of Eqs. (3) and (6), the exciton state derived from νth hole and μth electron subband can be written as

$$\Psi_{\rm ex}^{\mu\nu}(\rho,\varphi,z_e,z_h)=\sum_{k,\theta} G_{\mu\nu}(k,\theta)\exp[ik\rho\cos(\theta-\varphi)]f_\mu(z_e)U_0(\alpha_\nu\exp(-i\theta),\beta_\nu,\gamma_\nu\exp(i\theta),\delta_\nu\exp(i2\theta))^T , \tag{7}$$

where $G_{\mu\nu}$ as a general function of $\mathbf{k}(k,\theta)$, periodic in θ, can be expressed generally as

$$G(k,\theta)=\sum_l G^l(k)\exp(il\theta) . \tag{8}$$

It can be shown that exciton states associated with different l in the envelope function are not coupled by the Hamiltonian (4), so, without any loss of generality, only one term in (8) need be retained. Integrating with respect to θ in (7), the exciton state can be expressed as

$$\begin{aligned}\Psi_{\rm ex}^{\mu\nu}(\rho,\varphi,z_e,z_h)&=\sum_k G^l(k)f_\mu(z_e)U_0 2\pi\begin{pmatrix}\alpha_\nu(k,z_h)e^{i(l-1)(\varphi+\pi/2)}J_{l-1}(k\rho)\\ \beta_\nu(k,z_h)e^{il(\varphi+\pi/2)}J_l(k\rho)\\ \gamma_\nu(k,z_h)e^{i(l+1)(\varphi+\pi/2)}J_{l+1}(k\rho)\\ \delta_\nu(k,z_h)e^{i(l+2)(\varphi+\pi/2)}J_{l+2}(k\rho)\end{pmatrix}\\ &\equiv(\Psi_{l-1,3/2},\Psi_{l,1/2},\Psi_{l+1,-1/2},\Psi_{l+2,-3/2})S ,\end{aligned} \tag{9}$$

where $J_l(x)$ is the lth order Bessel function of argument x and S is the spin function of the electron. The second line of (9) is introduced merely to indicate the angular momenta involved, where the first suffix denotes the in-plane orbital angular momentum and the second suffix denotes the j value for the spinor components.

For variational calculation, the total energy can be divided into an effective kinetic energy term $E^{\rm kin}$ and a Coulomb term $E^{\rm Coul}$:

$$\begin{aligned}\frac{\langle\Psi_{\rm ex}|H_{\rm ex}|\Psi_{\rm ex}\rangle}{\langle\Psi_{\rm ex}|\Psi_{\rm ex}\rangle}&=\frac{\langle\Psi_{\rm ex}|H_e+H_h|\Psi_{\rm ex}\rangle}{\langle\Psi_{\rm ex}|\Psi_{\rm ex}\rangle}\\ &\quad+\frac{\langle\Psi_{\rm ex}|V_{\rm Coul}|\Psi_{\rm ex}\rangle}{\langle\Psi_{\rm ex}|\Psi_{\rm ex}\rangle}\\ &=E^{\rm kin}+E^{\rm Coul} .\end{aligned} \tag{10}$$

As the electron- and hole-subband wave functions making up the exciton wave function are eigenfunctions of H_e+H_h, with eigenvalues given by the subband dispersion curves, the effective kinetic energy term $E^{\rm kin}$ is directly derived from the subband dispersion curves. The Coulomb term depends, however, essentially on the detailed spatial distribution of the exciton wave function. Referring to the exciton wave function (9), clearly if a component is associated with the Bessel function $J_0(k\rho)$, it will be most effective in lowering the Coulomb term. However, even with free choice of l, (9) permits at best only one of the four components to have a $J_0(k\rho)$. Thus for the ground state, we shall choose l so that the largest component, if such exists, has a Bessel function $J_0(k\rho)$. It turns out that, for a given subband, such a dominant component does exist. As we know, the exciton wave function is made up of electron and hole states within a limited range of k around $k=0$ (which is correlated with the spatial extension of the exciton). For a given subband, at $k=0$ the hole wave function reduces to a single component, actual calculations show that this component remains in fact the dominant component throughout the relevant range of k involved in actual excitons.

From (9), it is seen that if m_d is the j value of the dominant component, then with

$$l=-\tfrac{1}{2}+m_d \tag{11}$$

that component will have a Bessel function $J_0(k\rho)$. Thus for the ground state of HH1-CB1 exciton, $\Psi_{\rm ex,1s}^{\rm HH1\text{-}CB1}$, $m_d=-\frac{3}{2}$, and $l=-2$; for $\Psi_{\rm ex,1s}^{\rm LH1\text{-}CB1}$, $m_d=\frac{1}{2}$, and $l=0$.

The assignment of l by (11) is the analog of an s state. For an excited state of exciton $\Psi_{{\rm ex},nm}$, associated with quantum numbers of $2D$ hydrogenic atom n,m, we derive the l value from the angular momentum quantum number m

$$l=-\tfrac{1}{2}+m_d+m . \tag{12}$$

The exciton state thus obtained corresponds to a total angular momentum quantum number given by

$$M_z=m-m_d+s , \tag{13}$$

for the quasi-2D exciton. By analyzing the symmetry of the exciton state constructed in this way, we find that the factor $(\Psi_{-3,3/2},\Psi_{-2,1/2},\Psi_{-1,-1/2},\Psi_{0,-3/2})$ contained in $\Psi_{ex,1s}^{HH1\text{-}CB1}$ has Γ_7 symmetry and $(\Psi_{-1,3/2},\Psi_{0,1/2},\Psi_{1,-1/2},\Psi_{2,-3/2})$ of $\Psi_{ex,1s}^{LH1\text{-}CB1}$ has Γ_6 symmetry, whereas if we had left out the angular factors in the hole wave function (7), the factor of $(\Psi_{0,3/2},\Psi_{0,1/2},\Psi_{0,-1/2},\Psi_{0,-3/2})$ would be a mixture of two different representations Γ_6 and Γ_7 and could not be assigned a quantum number M_z.

For variational calculation of the exciton states, in analogy to 2D hydrogenic radial function $\Phi_{nm}(\rho)$, the envelope function of an nm-state exciton is assumed to have the following form:

$$G^{nm}(k)=\int \rho\, d\rho\, \Phi_{nm}(\rho)J_m(k\rho)\ . \tag{14}$$

Thus

$$G^{1s}(k)=\alpha(\alpha^2+k^2)^{-1.5}\ ,$$

$$G^{2s}(k)=\alpha(k^2-\alpha^2)(\alpha^2+k^2)^{-2.5}\ ,$$

$$G^{2p}(k)=k\alpha(\alpha^2+k^2)^{-2.5}\ ,$$

and

$$G^{3d}(k)=k^2\alpha(\alpha^2+k^2)^{-3.5}\ ,$$

where α will be taken as a variational parameter. In order to obtain a more accurate value for E_{1s}^{ex}, an envelope function of $G^{1s}(k)=\alpha(\alpha^2+k^2)^{-\beta}$ with two variational parameters α and β are used.

As a check on the accuracy of the two-band model, we have carried out variational calculations on the basis of combining the three lowest-lying excitonic series, i.e., HH1-CB1, LH1-CB1, and HH2-CB1 to form a variational wave function $\Psi_{ex}=\sum_i c_i\Psi_{ex}^i$. It should be pointed out that, as apparently ignored in previous research, coupling between different excitonic series occurs only between exciton states with the same phase factor $\exp(il\varphi)$ for their corresponding spinor components. Thus in order to investigate the effect of coupling to the HH1 and HH2 excitonic series on the LH1 exciton E_{1s}^{ex}(LH1-CB1), the variational function needs only to include the excitons $\Psi_{ex,3d}^{HH1}$ and $\Psi_{ex,2p\_}^{HH2}$; there is no coupling to the ground-state excitons.

IV. RESULTS

A. Binding energies of ground-state excitons

Figure 2 presents the results of theoretical calculations designed to demonstrate the different effects of valence band hybridization on the binding energies of the ground-state HH1-CB1 and LH1-CB1 excitons. The results were calculated for GaAs-$Ga_{0.75}Al_{0.25}As$ quantum wells with well widths ranging from 30 Å to 200 Å (barrier width is fixed at 150 Å in this instance). In the figure E_{1s}^{ex} calculated with three different models is presented as a function of well widths. Approximation I represents results calculated with the parabolic-hole-subband model, similar to that of Greene and Bajaj. II represents results calculated with a model, essentially similar to Ref. 7 as explained earlier, which takes account of the nonparabolic subbands resulting from valence band hybridization. The third set of results are

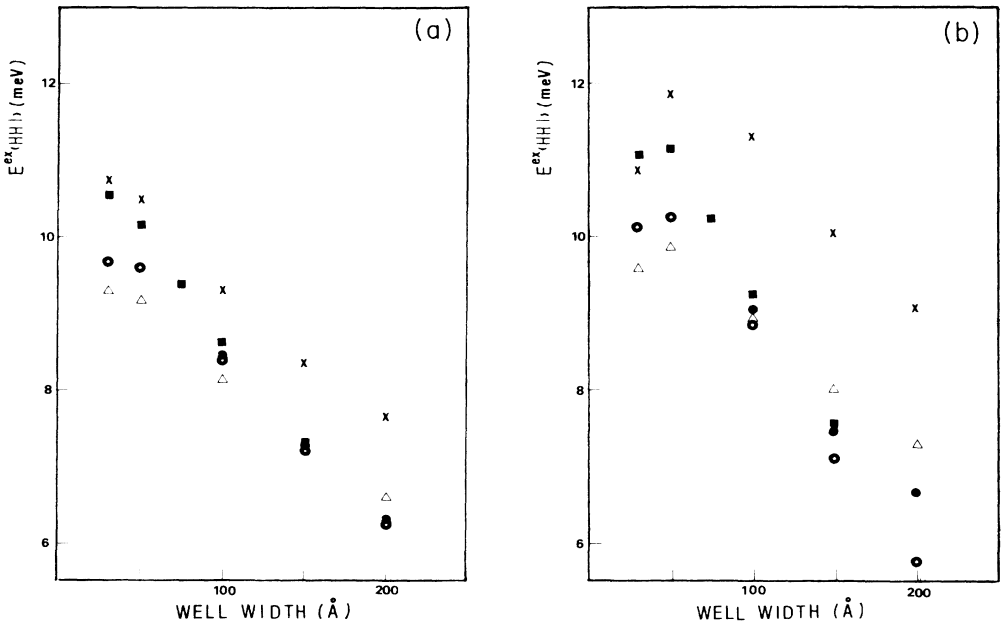

FIG. 2. Exciton binding energies vs well widths in GaAs-$Ga_{0.75}Al_{0.25}As$ quantum well calculated in five different models: △, Approx. I; ×, Approx. II; ○, including both aspects of the effect of hole hybridization within two-band model; ● as ○, but beyond two-band model; ■, as ●, but the nonparabolicity of the CB electron is involved. (a) E_{1s}^{ex}(HH1-CB1); (b) E_{1s}^{ex}(LH1-CB1).

calculated with the model which takes proper account of the effect of valence band hybridization on both E^{kin} and E^{Coul}.

A comparison between the results of I and II clearly demonstrates that the nonparabolicity of the hole subbands results in decreased E^{kin} and increased E_{1s}^{ex}, already emphasized in Refs. 7 and 8. This enhancement of E_{1s}^{ex} is not sensitive to well width, because the hole dispersion changes little relative to $1/m_e^*$. The only exception is E_{1s}^{ex}(LH1-CB1) for narrow well with $L=30$Å, where the LH1 effective mass near $k=0$ becomes positive showing up as a lesser enhancement of E_{1s}^{ex}.

From the figure, it is seen that the effect of the valence band mixing through E^{Coul} is to reduce the exciton binding energy. The reason is that while the dominant component varies as $J_0(k\rho)$ like an s state, the other components behave like $J_m(k\rho)(m\neq 0)$, which represents a more extended radial distribution in the xy plane and thus reduces the Coulomb energy. In Fig. 3 the wave function square contributed by all four components of the 1s state LH1 exciton and that contributed by only the dominant component are shown as functions of ρ (at a given z_h), for comparison.

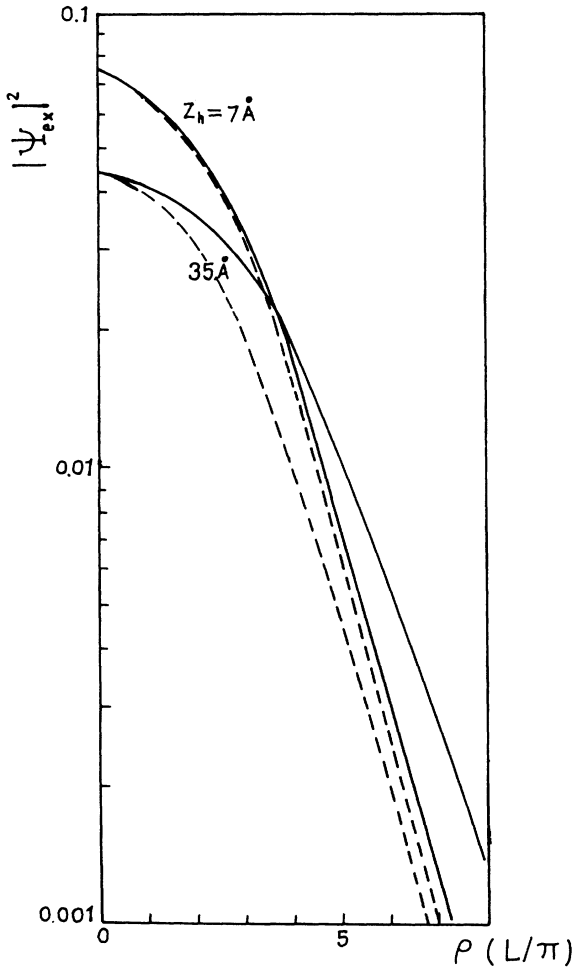

FIG. 3. Wave function square of the 1s state of LH1-CB1 exciton as function of ρ at given z_h in a QW of $L=150$ Å. Solid curves include all four components; dashed curves, only the dominant component is involved.

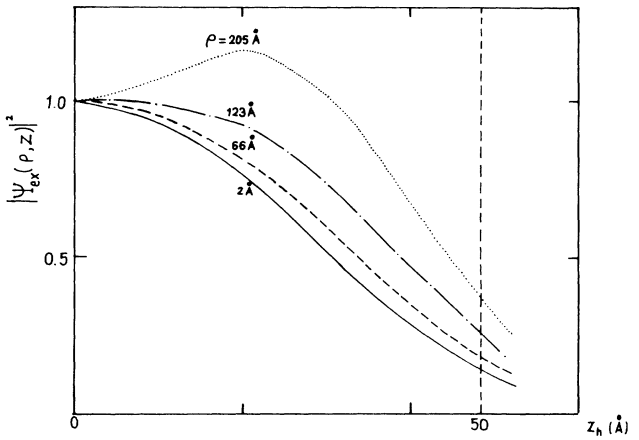

FIG. 4. Wave function square of the 1s state of LH1-CB1 exciton as function of z_h for given ρ in a QW of $L=100$ Å (taking the value at $z_h=0$ as a unit). The vertical line represents the position of the QW interface.

The effect of complex subband on E^{Coul} manifests itself not only in the change of the excitonic in-plane distribution, but also in the interdependence between the excitonic motion parallel and perpendicular to the xy plane. Thus the farther the hole is away from the well center, the more extended is the exciton in the xy plane (Figs. 3 and 4); or, with the increase of ρ, the excitonic distribution along z direction becomes more extended. Such effects act to further reduce E_{1s}^{ex}.

In contrast to the effect of nonparabolicity, the effect on E^{Coul} of hole hybridization is sensitive to well widths. This is because the degree of valence band hybridization, and hence the general magnitudes of the nondominant spinor components of the exciton, depends essentially on kL. So for thicker wells with larger L, these components become relatively more important and modify more strongly the Coulomb energy, especially for $\Psi_{\text{ex},1s}^{\text{LH1}}$ which contains a larger component of $\Psi_{-1,3/2}$.

The results shown in Fig. 2 show clearly that the two aspects of the effect of valence band hybridization on the binding energy of the ground-state excitons act to cancel each other. In narrower wells, the effect of subband nonparabolicity dominates and in sufficiently wide wells, the effect through E^{Coul} dominates.

B. Binding energies of excited state of excitons

Just as the case for E_{1s}^{ex}, there is a critical value of well width L_c at which the binding energy of the exciton reaches a maximum value. But L_c of the excited state is much larger than L_c of the ground state and L_c of the $2p$ state is larger than L_c of the $2s$ state (cf. Fig. 5). The common reason lies in the fact that the compression of the excitonic wave function along the z-direction is less effective in the enhancement of E^{ex} when the exciton is

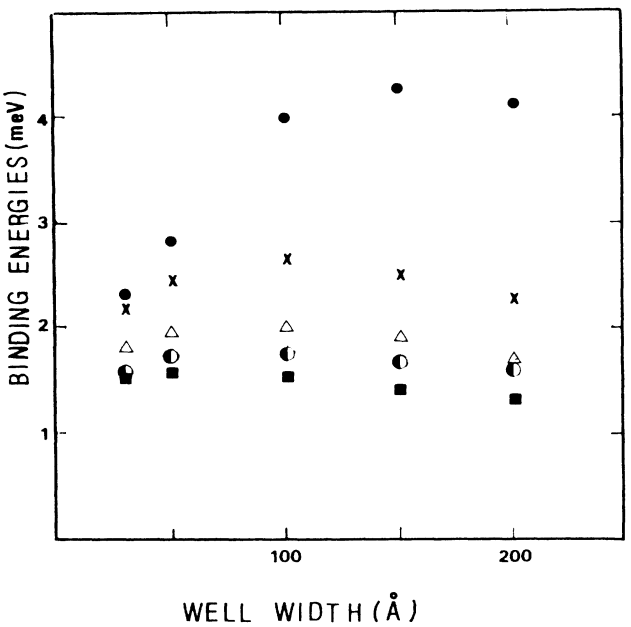

FIG. 5. Exciton binding energies of excited states as a function of well widths: ●, $E^{ex}_{2p_+}$(LH1-CB1); ×, $E^{ex}_{2p_-}$(LH1-CB1); △, E^{ex}_{2s}(LH1-CB1); ◐, E^{ex}_{2p}(HH1-CB1); ■, E^{ex}_{2s}(HH1-CB1).

more extended in the xy plane. Another phenomenon connected with the fact is $E^{ex}_{2p} > E^{ex}_{2s}$. We know that $E_{2p} = E_{2s}$ for $2D$ hydrogenic atoms. As the $2s$ state is more concentrated near $\rho \sim 0$ compared with $2p$ state, clearly in going over from $2D$ hydrogen to $2D$ exciton in QW, the reduction of Coulomb energy due to extension in z direction will be pronounced in the case of $2s$ exciton as compared with $2p$ exciton, resulting thus in a lesser binding of the $2s$ exciton than E^{ex}_{2p}. We predict that with L narrowing the quasi-$2D$ exciton becomes more $2D$-like and E^{ex}_{2s} and E^{ex}_{2p} should become equal in the limit if the spread of the wave function into the barrier is negligible. Our calculation suggests its validity. For example, $E^{ex}_{2p} - E^{ex}_{2s}$ is of only 0.06 meV for HH1 exciton in a well of $L = 30$ Å.

In contrast to the case of ground-state excitons, both aspects of the effect due to valence band coupling act to increase the binding energies of the p-state and d-state excitons. The reason is simple. As in these excited states, while the dominant component of the spinor varies as $J_\rho(k\rho)$, such as $J_1(k\rho)$ (taking p_+ state as an example), there exists another component behaving like $J_0(k\rho)$, which is spatially less extended compared with the dominant component and leads to stronger binding (i.e., compared with models with effectively a single component). The hybridization also results in a possible splitting of $2p_+$ and $2p_-$ state, if, for instance, the $\Psi_{0,3/2}$ component of $\Psi^{LH1}_{ex,2p_+}$ is much larger than $\Psi_{0,-1/2}$ component of $\Psi^{LH1}_{ex,2p_-}$. Since $\psi_{h,LH1}$ contains a comparable first component with the dominant part, $E^{ex}_{2p_+}$(LH1) is obviously larger than $E^{ex}_{2p_-}$(LH1). There is no such splitting for $2p$ state of HH1 exciton as the third component of $\psi_{h,HH1}$ is negligible.

TABLE I. Comparison of binding energies of the $1s$-state exciton calculated within two-band model with that calculated beyond two-band model.

Well width (Å)	E^{ex}_{1s}(HH1) (meV) Two-band	Beyond	E^{ex}_{1s}(LH1) (meV) Two-band	Beyond
200	6.23	6.31	5.76	6.64
150	7.19	7.25	7.10	7.47
100	8.42	8.44	8.86	9.03

C. Beyond two-band model

The effect on E^{ex}_{1s}(HH1-CB1) of coupling with $3d$ state of LH1-CB1 exciton is shown in Table I. The data indicate that the two-band model is a good approximation for the calculation of E^{ex}_{1s}(HH1).

In the case of the $1s$ state of LH1-CB1 exciton, the effect of Fano resonance[11] is neglected, only coupling between bound states from different excitonic series is considered. The table shows significant deviations in the case of E^{ex}_{1s}(LH1) when $L \gtrsim 150$ Å, which is due mainly to the coupling between $\Psi^{LH1}_{ex,1s}$ and $\Psi^{HH2}_{ex,2p_+}$. An interesting instance about this coupling is the ground state of LH1-CB1 exciton in a well of $L = 200$ Å. Using the two-band model with energy zero taken at the HH1-CB1 free-carrier edge, the calculated excitonic level of E^{ex}_{3d}(HH1-CB1) is at -0.63 meV, E^{ex}_{1s}(LH1-CB1)$=-0.39$ meV, and $E^{ex}_{2p_+}$(HH2-CB1)$=4.5$ meV. (No Fano resonance for LH1 exciton occurs in this case.) When couplings between these states are turned on, the two lowest levels and wave functions are found to be as follows: $E_1 = -1.27$ meV, $\Psi_{ex} = 0.82\Psi^{LH1}_{ex,1s} + 0.49\Psi^{HH1}_{ex,3d} + 0.29\Psi^{HH2}_{ex,2p_+}$, $E_2 = -0.43$ meV, $\Psi_{ex} = -0.46\Psi^{LH1}_{ex,1s} + 0.87\Psi^{HH1}_{ex,3d} - 0.15\Psi^{HH2}_{ex,2p_+}$. It is the coupling between $\Psi^{LH1}_{ex,1s}$ and $\Psi^{HH2}_{ex,2p_+}$ that pushes E^{ex}_{1s}(LH1) down below E^{ex}_{3d}(HH1).

V. DISCUSSION AND CONCLUSION

Since no adjustable parameters are involved in this calculation, the only sources of inaccuracy are the following approximations: (1) the asumption of hole subband isotropy, (2) the same effective mass parameter and dielectric constant used for both the well and barrier materials, (3) neglect of Fano resonance, and (4) parabolic conduction band for the electron.

Since the subbands are nearly isotropic in the region of interest near $k = 0$ and the dispersion curves with isotropy approximation seems to be the average of the real dispersion curves along the [100] and [110] directions when k is large (cf. Fig. 1), the error due to isotropic dispersion is 2% at most according to our estimates. Since the physical parameters of GaAs and GaAlAs are not too different and the exciton wave functions are primarily confined within the well, the second approximation above should not cause large errors. A detailed investigation on the effect due to Fano resonance is still in progress, but according to Ref. 8, it is not expected that

our main conclusions will be affected. Finally, the parabolic band approximation for the conduction electron may increase E_{1s}^{ex} by an amount of the order of meV for narrower well widths. As following $\mathbf{k}\cdot\mathbf{p}$ perturbation theory, the nonparabolic electron effective mass is given by[12]

$$m_e^* = (0.0665 + 0.0436E + 0.236E^2 - 0.147E^3)m_0$$

with E evaluated from the CB edge in units of eV. The value of E_{1s}^{ex} calculated on this basis as a function of L is also depicted in Fig. 2.

The existing experimental data on E_{1s}^{ex} are indirect and divergent.[13–16] However, as the photoconductivity measurements made by Rogers *et al.* were carried out in steady magnetic fields down to 2.5 T, permitting thus a more exact determination of E_{1s}^{ex} by linear extrapolation,[15] we have compared our results with their data (cf. Table II). In view of the experimental uncertainty and the approximations used in our calculations, the agreement between experiments and theory is fairly good.

In conclusion, the complex nature of the hole subbands due to intermixing of heavy and light holes affects intricately the exciton spectra in quantum wells. The effect of valence band hybridization on the Coulomb interaction is generally comparable in magnitude with the effect of hole-subband nonparabolicity on the effective kinetic energy. The different orbital angular momenta associated with the spinor components of the exciton wave function have the effect of reducing the binding energies of the s states and of increasing the binding energies of the p and d states. While such effects dominate in quantum wells of sufficient widths, the effect of subband nonparabolicity on both hole and electron always acts to increase the exciton binding energies and dominates for sufficiently narrow quantum wells. The two-band model is fairly good for calculating E_{1s}^{ex}(HH1), but produces significant errors for E_{1s}^{ex}(LH1) in the wider wells.

TABLE II. Calculated binding energies of the 1s-state exciton in quantum wells of GaAs-$Ga_{0.65}Al_{0.35}As$ compared with experiments (Ref. 15).

Well width (Å)	E_{1s}^{ex}(HH1) (meV) Expt.	Theory	E_{1s}^{ex}(LH1) (meV) Expt.	Theory
75	10	9.67	11	11.05
110	8	8.59	9	9.30

ACKNOWLEDGEMENT

This work was supported by the Science Fund of the Chinese Academy of Sciences.

*Department of Physics and Measurement Technology, University of Linköping, Linköping, Sweden, and Institute of Semiconductors, Academia Sinica, China.

[1]R. L. Greene, K. K. Bajaj, and D. E. Phelps, Phys. Rev. B **29**, 1807 (1984).
[2]Y. C. Chang and J. N. Schulman, Phys. Rev. B **31**, 2069 (1985).
[3]Y. C. Chang and J. N. Schulman, Appl. Phys. Lett. **43**, 536 (1983).
[4]R. C. Miller, A. C. Gossard, G. D. Sanders, Yia-Chung Chang, and J. N. Schulman, Phys. Rev. B **32**, 8452 (1985).
[5]H. Tang and K. Huang, Chin. J. Semicond. **8**, 1 (1987).
[6]J. M. Luttinger and W. Kohn, Phys. Rev. **97**, 869 (1956).
[7]G. D. Sanders and Y. C. Chang, Phys. Rev. B **32**, 5517 (1985).
[8]D. A. Broido and L. J. Sham, Phys. Rev. B **34**, 3917 (1986).
[9]H. J. Lee, L. Y. Juravel, J. C. Wooley, and A. J. Springthorpe, Phys. Rev. B **21**, 659 (1980).
[10]R. C. Miller, D. A. Kleinman, and A. C. Gossard, Phys. Rev. B **29**, 7085 (1984).
[11]U. Fano, Phys. Rev. **124**, 1866 (1961).
[12]S. Chaudhuri and K. K. Bajaj, Phys. Rev. B **29**, 1803 (1984).
[13]R. C. Miller, D. A. Kleinman, W. T. Tsang, and A. C. Gossard, Phys. Rev. B **24**, 1134 (1981).
[14]J. C. Maan, G. Belle, A. Fasolino, M. Altarelli, and K. Ploog, Phys. Rev. B **30**, 2253 (1984).
[15]D. C. Rogers, J. Singleton, R. J. Nicholas, C. T. Foxon, and K. Woodbridge, Phys. Rev. B **34**, 4002 (1986).
[16]B. A. Vojak, N. Holonyyak Jr., D. W. Laidig, K. Hess, J. J. Coleman, and P. D. Dapkus, Solid State Commun. **35**, 477 (1980).